Appl Phys A (2008) 92: 897–902
DOI 10.1007/s00339-008-4632-x

Applied Physics A
Materials Science & Processing

Near-damage threshold femtosecond laser irradiation of dielectric surfaces: desorbed ion kinetics and defect dynamics

Florenta Costache · Sebastian Eckert · Jürgen Reif

Received: 12 October 2007 / Accepted: 9 April 2008 / Published online: 13 June 2008

Abstract We study the modification of fluoride single crystals after irradiation with femtosecond laser pulses for a range of incident intensities from well below to near damage threshold. The behavior of the desorbed positive ion yields, as analyzed by time-of-flight mass spectrometry, is corroborated with temporal characteristics of radiation induced defects in fluorides.

The ion yield evolution upon repetitive irradiation (incubation) exhibits the typical reduction of the multi-shot damage threshold with increasing number of pulses. The experimental data point towards an exponential growth of the transient defect density as the origin of this effect. On the other hand, measurements of the time decay of transient defect fluorescence inside the transparent sample show that the defect lifetime may be even longer than tens of milliseconds.

To account for the incubation and the increase of the radiation-target coupling efficiency, a model relating the defect lifetime to a pulse-by-pulse accumulation of transient defects is presented, based on a calculation of the free electron density.

PACS 79.20.Ds · 82.80.Ms · 61.80.Ba

1 Introduction

Intense femtosecond laser pulses give rise to a strong perturbation in the interaction volume of a wide bandgap material in the ultra-short interaction time. The irradiated material undergoes lattice destabilization and particles are likely desorbed from the surface.

Experimental [1–5] and theoretical [6] works have indicated that particle desorption, (well) below the macroscopic damage threshold, is primarily triggered by electrostatic repulsion between neighboring positive ions from within a highly charged near-surface region, almost depleted of electrons (Coulomb explosion).

Experiments on fluorides materials irradiated with femtosecond laser pulses have shown that at intensities in the range of 10^{10}–10^{12} W/cm^2, the excitation can provoke a strong emission of electrons as well as positive and negative ions [1, 2]. Furthermore, the experiments indicated that the electron and ion yields exhibit a strong correlation in their emission kinetics [1, 3]. The presence of defects could provide a significantly 'shrinkage' in the material bandgap by filling intermediate states. A lower order ionization process could occur via these states [7, 8], facilitating therefore both electron and ion emission.

Defects in fluorides are known to readily form after electron or ion bombardment or laser irradiation [9–11]. Color centers and metallic colloids likely occur after prolonged irradiation at moderate intensities and could be visible due to a typical coloration inside the transparent sample. Defects accumulate at the surface upon repetitive laser irradiation (incubation).

Upon multiple femtosecond laser pulse irradiation the defect accumulation could basically be both associated with and accompanied by surface positive charges. In the present work, we report on additional experiments meant to improve the understanding of the relevant processes for the incubation phenomenon in fluoride materials irradiated with femtosecond laser pulses. For explaining this process, we propose an approach derived from measurements of surface charging with an increasing number of pulses. We believe

F. Costache (✉) · S. Eckert · J. Reif
Brandenburg University of Technology and Cottbus JointLab
IHP/BTU, Konrad-Wachsmann-Allee 1, 03046 Cottbus, Germany
e-mail: costache@physik.tu-cottbus.de

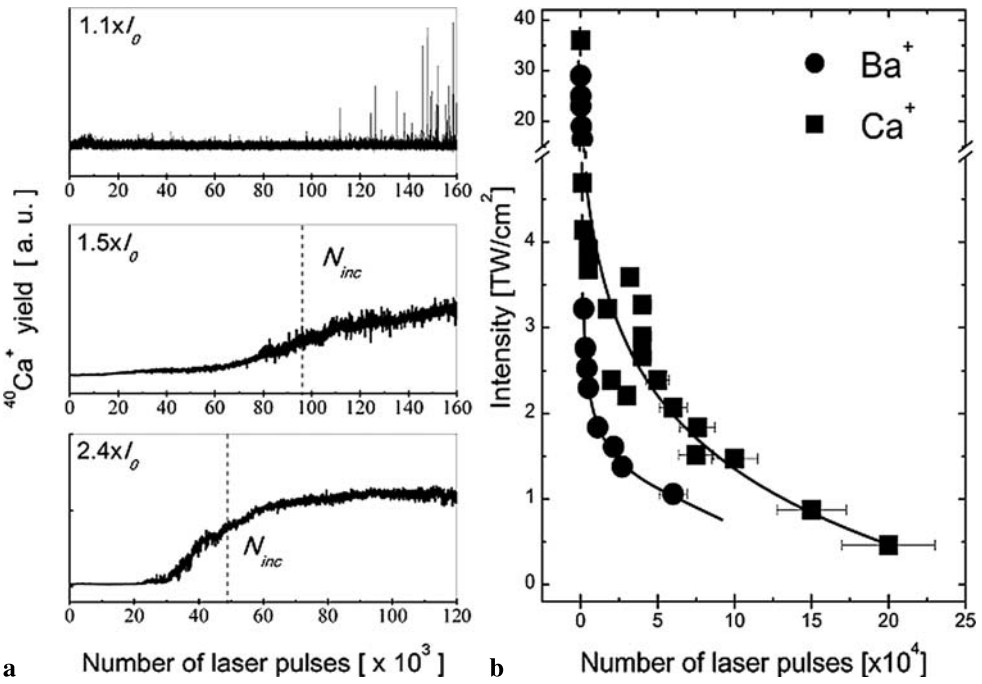

Fig. 1 Incubation behavior of Ca^+ ions from CaF_2 (**a**), as selected from the ToF spectra, at different laser intensities indicated in the panels ($I_0 = 1$ TW/cm^2). (**b**) The 'incubation' data for Ca^+ and Ba^+ yields, i.e. the intensity dependence on the number of 'incubative' pulses N_{inc}. The solid lines represent exponential decay fits on the experimental data

that defects play a determinant role in the incubated dynamics. We attempt here to describe this effect: we assume that a pulse-by-pulse accumulation of defects on the surface occurs if there is a defect with a lifetime of about the time interval between successive pulses.

2 Experimental

We carried out experiments to analyze the ion desorption kinetics and defect dynamics from freshly cleaved, single crystals of $BaF_2(111)$ and $CaF_2(111)$ after femtosecond laser excitation.

For detection and analysis of the desorbed positive ion yields, we used a linear time-of-flight (ToF) mass spectrometer (1.5 m drift length) oriented normal to the target. An extraction field of about 1000 V/cm was applied between the target and the entrance aperture of the spectrometer. The ToF spectrometer is equipped with an MSP detector and a pair of electrostatic lenses of cylindrical geometry to maximize the ion yield. ToF positive ion spectra were visualized on a 400 MHz oscilloscope (LeCroy) and analyzed using boxcar gated integrators. The laser system used was a Ti:Sapphire CPA laser system (Spectra Physics), ∼120 fs pulses of 800 nm, <0.5 mJ energy per pulse, 1 kHz repetition rate, horizontally polarized. The targets were cleaved in air and immediately transferred into an ultra-high vacuum chamber (base pressure $<10^{-9}$ mbar).

In these experiments, we varied the laser intensities in the range of 10^{11}–10^{14} W/cm^2. Measurements of the positive ion yields were performed under multi-shot mode N-on-1.

Laser induced fluorescence (LIF) was detected at laser intensities near the single pulse damage threshold (∼30 TW/cm^2 for $CaF_2(111)$ and ∼20 TW/cm^2 for $BaF_2(111)$ [12]), where the fluorescence intensity, its emission characteristics and lifetime could be easily detected. A Ti:Sapphire CPA laser system of up to 2 mJ energy per pulse and 20 Hz repetition rate was used for carrying out these measurements. Single 120 fs pulses (800 nm) were selected from the 20 Hz pulse train by means of an electronic shutter.

An ICCD camera of nanosecond resolution (Hamamatsu C4346-01) was used for the fluorescence detection. The gated signal from the camera was collected at a controlled time delay with respect to the laser pulse. The LIF emission ranges were analyzed by using a set of band-pass filters.

3 Results and discussion

3.1 Incubation: the role of defects

First, we examined the ion yield evolution after repetitive irradiation with 120 fs laser pulses. This was done by selecting from a time-of-flight spectrum the ion peak of interest and integrating it for each laser pulse. In Fig. 1a, we present the dependence of Ca^+ yields from CaF_2 on the number of laser pulses. It can be easily observed that after a certain number of accumulated (incubative) pulses, the ion yield increases until it reaches a quasi-steady regime. At further irradiation no significant change is observed, resembling a saturation effect. On the other hand, the amplitude of

the 'saturated' ion signal increases nonlinearly with increasing intensity; this is expected to happen due to the nonlinear photoionization.

It is easy to notice that the number of incubative pulses to reach the 'saturated' ion yield, becomes smaller and smaller with increasing intensity.

This appears to support a common interpretation for the incubation effect: the first laser pulses create defects at the surface, which increase in number at further irradiation until the defect density locally 'saturates'. The interpretation can hold as well if we consider a pulse-to-pulse surface positive charge accumulation such as in the Coulomb explosion model.

We attempt to qualitatively analyze this result as follows: we assume a characteristic number N_{inc} as the mean value between an average minimum and maximum ion yield (see Fig. 1a). We find that the intensity $I(N_{\mathrm{inc}})$ decays exponentially with N_{inc}, both for Ca^+ from CaF_2 and for Ba^+ from BaF_2 (Fig. 1b).

Our result shows that the number of pulses necessary to reach a critical defect density (accompanied perhaps by a local saturation in surface charging), for substantial ion emission, decreases with increasing laser intensity. Here $I(N_{\mathrm{inc}}) \propto \exp(-aN_{\mathrm{inc}})$, where a is a constant.

On the other hand, we basically observe the usual effect of reduction of the damage threshold intensity for multipulse irradiation, due to radiation absorption enhancement at the defects sites.

We need to note here that from the definition of N_{inc}, the result from Fig. 1b characterizes only the regime with a 'saturated' defect density, i.e. the regime of quasi-steady ion yield. It is evident that for intensities close to damage threshold, N_{inc} should be small.

We have previously shown that if irradiation (at 1 kHz repetition rate) is ceased for tens of milliseconds, further irradiation will be characterized by further incubation [1]. The irradiation should be accompanied by defect creation (or positive charge accumulation). Our observation is that the time until the next irradiation is a determining factor for recommencing incubation. We assume that this time is related to the creation and relaxation of defects. To understand this, we further performed measurements of the temporal characteristics of the laser induced fluorescence.

3.2 Laser induced defects in fluorides

We evaluate the defect relaxation time by analyzing the remaining fluorescence after the laser pulse ceased. The experimental set-up for the detection of LIF from BaF_2 and CaF_2 is presented in Fig. 2a. The inset shows an image of the typical fluorescence emission trace in a fluoride target. Here, a single pulse hits the surface and generates a plasma plume and fluorescence emission in the interaction volume.

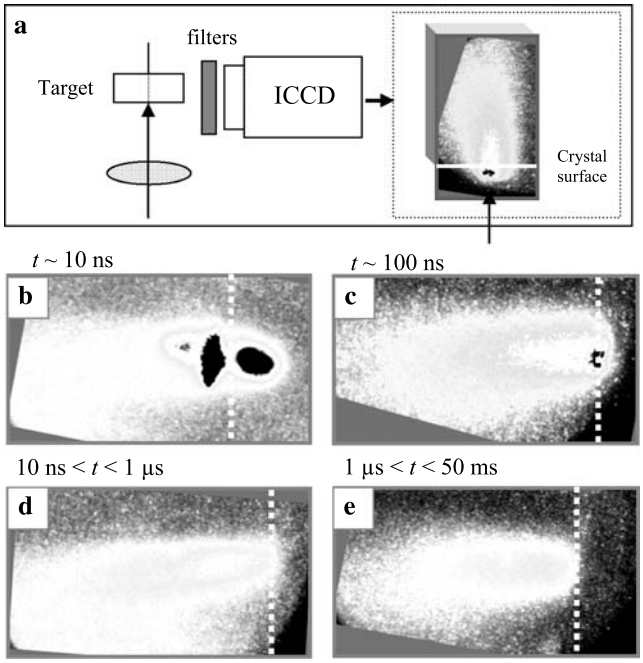

Fig. 2 (**a**) Schematic of the experimental set-up for laser induced fluorescence measurements; the inset presents an image seen by the ICCD camera, in a cross-section of a transparent crystal; the laser pulse gives rise to fluorescence emission in the interaction volume. Images of plasma radiation and fluorescence emission in a $BaF_2(111)$ target irradiated by a single 120 fs laser pulse, at 800 nm and time delays as indicated: (**a**) plasma formation and expansion in 10 ns; (**b**, **c**) F(I) fluorescence detected and integrated between 10 ns to 1μs; (**d**) F(II) fluorescence detected and integrated between 1 μs to 50 ms delay time to the laser pulse. The laser pulse hits the crystal surface from the right side; the surface is represented by dotted lines. (Laser intensity: 1.1×10^{15} W/cm^2)

From the emission spectrum and detection time interval, we distinguish two main fluorescence ranges: a more intense short lifetime fluorescence band F(I) in the near-UV and a red-shifted less intense fluorescence band F(II) of a longer lifetime. Images of single laser pulse induced plasma radiation and fluorescence emission from $BaF_2(111)$, for various delay times with respect to the laser pulse, are presented in Fig. 2b–e.

Both fluoride materials investigated exhibit fluorescence emission upon femtosecond laser pulse irradiation. In Table 1, we summarize the fluorescence emission ranges and the corresponding detection time intervals.

From the data we infer that microsecond lifetime defects emitting the fluorescence (FI) could be self-trapped excitons (STE). STEs are well known to develop in fluorides and other transparent crystals after UV femtosecond laser irradiation [13]. As indicated in [9], STEs can decay over several intermediate states, reaching an overall lifetime of >1 μs. A fluorescence detected at around 278 nm with a lifetime of $\sim$1 μs has been associated to the decay of an STE [9].

The much longer lifetime F(II) fluorescence could indicate a surface F-center, which has been shown to decay in

Table 1 Laser induced fluorescence from $BaF_2(111)$ and $CaF_2(111)$ irradiated by single pulses at 5×10^{14} W/cm^2 intensity: emission ranges and their detection time intervals

	Emission ranges (nm)	Detection time interval, t_{LIF}
BaF_2	F(I): 300–400 nm	~1 μs
	F(II): 400–465 nm	>50 ms
CaF_2	F(I): 300–400 nm	≥100 ns
	F(II): 500–600 nm	>50 ms

about 50 ms [10] or much longer [11]. It is to be shown in the next subsection that such defects are assumed here to be responsible for the incubation effect observed.

3.3 Incubation model

We attempt to model the effect of incubation based on our experimental results and existing models for dielectric surface damage induced with a femtosecond laser.

It is known that the primary response of a wide bandgap material to ultra-short laser pulse irradiation is multi-photon absorption and generation of free electrons both in the conduction band or emitted out of the target. It is generally assumed that an intense single pulse laser induces damage in a dielectric material when the free (conduction band) electron density reaches a critical density (plasma critical density—$n_c \sim 10^{21}$ cm^{-3} at 800 nm—or just below it [14]). A pulse-to-pulse increase in the excited electron density and multi-pulse laser damage presumably occurs if the relaxation process is carried out across defect states with an effective decay time comparable to or longer than the inter-pulse time interval. Based on this assumption, in the following we calculate the temporal evolution of the free electron density, taking CaF_2 as a case study.

First, we assume that the conduction band electron density builds up by band-to-band multiphoton ionization, mediated by defect states located within the bandgap. We apply a similar rate equation to that proposed in [15]. Although it is unlikely to happen at intensities below the threshold, for the sake of completeness, we also consider avalanche ionization as a source of excited electrons. Our main approximation is that ionization occurs across a defect state located near the conduction band edge, so that this can be an ionization/recombination bottleneck state. Hence, the ionization from this defect state and the return back to this state is assumed to be fully balanced and happening in a time much shorter than the inter-pulse time, i.e. its contribution to the remaining electron density at the beginning of the next pulse is taken to be negligible. On the other hand, we consider the relevant defect state to have a long recombination lifetime. We take into the rate equation only the ionization across and relaxation of these defect states. Additionally, we neglect losses through bulk diffusion or electron emission out of the target.

In CaF_2 with a bandgap of $E_g \sim 10$–12 eV,[1] a 7-photon process is most likely the band-band photoionization process. The long lifetime defect state is likely an F-center. Provided that this state lies at 8.3 eV from the valence band edge [16], for our excitation conditions, such a state could be filled by a 6-photon process. The ionization would correspond therefore to a single-photon process. For a sufficiently high density the direct band-band 7-photon ionization can be neglected compared to the $6+1$ ionization across the defect state.

Using the empirical method provided in [17], for the 7-photon ionization cross-section we obtain $\sigma_7 \sim 10^{-142}$ cm^{14} ps^6 and for a 6-photon ionization cross-section $\sigma_6 \sim 10^{-121}$ cm^{12} ps^5. We express the growth rate of the electron density by combining a multiphoton ionization and an avalanche rate with a recombination rate at a defect state. This reads

$$\frac{dn(t)}{dt} = \alpha \cdot I \cdot n(t) + PI - R_d. \tag{1}$$

Here, $PI = \sigma_7 \cdot (\frac{I}{h\nu})^7 \cdot N_s$ is the 7-photon ionization rate with N_s the solid atom density (for CaF_2, this is around $N_s \sim 2.4 \times 10^{21}$ at/cm^3). R_d is the recombination rate at the defect states:

$$R_d = \frac{dn_d}{dt} = -PI_d + \frac{n_d}{\tau_d}, \tag{2}$$

where $PI_d = \sigma_6 \cdot (\frac{I}{h\nu})^6 \cdot N_s$ is the 6-photon ionization rate for generation defect, and τ_d is the defect state decay time. In the calculation, the avalanche coefficient α in CaF_2 is taken to be ~ 2 cm^2/J as determined experimentally in [18].

For making the calculation easier, we considered a linear *growth* of a defect density with the number of pulses, in other words, we deal with the 'saturation' regime of the ion yield (cf. Fig. 1a). The electron density after a number of pulses N is calculated for a Gaussian pulse of a peak intensity I_0, using (1–2). This is

$$n(t, N) \approx [n_0 + N \cdot n_{0,d}] \times \exp\left[\frac{\alpha I_0 \tau_p}{4}\left(\frac{\pi}{\ln 2}\right)^{1/2} \mathrm{erf}\left(2\ln 2 \frac{t}{\tau_p}\right) - \frac{t}{\tau_d}\right], \tag{3}$$

where n_0 is the electron density due to photoionization, $n_{0,d}$ the defect density, and $\mathrm{erf}(x)$ is the standard error function.

It follows that, depending on τ_d, the incident intensity, and the number of pulses, a *residual* excited electron density may be present at the beginning of each subsequent

[1] The surface band-gap of cleaved $CaF_2(111)$ crystals is usually taken to be 10 eV, but it is known that the bulk bandgap could reach about 12 eV.

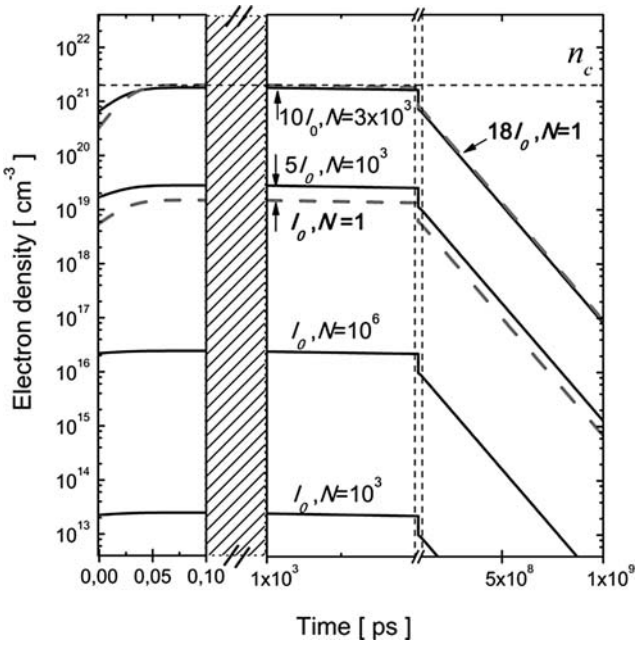

Fig. 3 Temporal evolution of the excited electron density at different incident intensities and number of laser pulses: $N = 10^3$ and 10^6 (*solid lines*). For 3×10^3 pulses of 10 TW/cm^2 the critical electron density is reached. Also shown is the temporal evolution of the excited electron density in a single pulse of different intensities (*dashed lines*)

pulse. This contributes ultimately to building-up the electron density. Figure 3 shows the temporal evolution of the conduction band electron density using (3), assuming that $\tau_p = 120$ fs and $\tau_d = 100$ µs, for different intensities and number of pulses.

We also calculate the temporal evolution of the electron density for a single laser pulse to yield $n_{\rm cr}$, where $n_{\rm cr} \sim 1.7 \times 10^{21}$ cm^{-3} at a laser wavelength of 800 nm. The corresponding intensity is found to be roughly the measured single-shot ablation threshold for CaF_2.

Such an effect could provide a residual electron density at the beginning of the next pulse. In fact, following these assumptions, for any intensity the critical density can be reached for a sufficient number of pulses.

4 Conclusions

The electron and ion yields increase nonlinearly with increasing irradiation intensity. An important enhancement occurs at repetitive irradiation, likely caused by a superior ionization probability across defect states located within the bandgap. Measurements of the fluorescence emission indicate that in laser-irradiated fluorides various defects are created, such as transient defects of 1 µs lifetime but also long-lived defects of a 50 ms lifetime. We have tried to model the influence of such defects on the electron and the corresponding ion yield, considering a strong corroboration in their emission characteristics. In our model, the initial assumption is that after the electrons are emitted out of the target the positive ion desorption occurs when a certain surface hole density is reached, at least locally.

A pulse-by-pulse increase in the surface defect density can potentially enhance the conduction band electron density, leading to photo-electron and consequently ion emission.

We discussed the excitation and recombination processes that may contribute to building-up of the electron density during the laser pulse, and its decay in between successive pulses, considering surface defects of a lifetime longer than the time interval between pulses (at a pulse repetition rate of 1 kHz). Hence, we show that if the created defects accumulate pulse by pulse, the excited electron density increases and so should do the corresponding hole density in the valence band. Further, by adding more pulses, the hole density, i.e. the positive ion density, continues to grow until positive ions form close to each other. The electrostatic repulsion between adjacent positive ions causes ions to be desorbed out of the target. Eventually the ion yield can reach a quasi-steady regime. For low intensities, the positive charge is localized at defect sites. With increasing intensity, the number of defects (absorbent sites) increases and possibly reaches a maximum near the damage threshold, where the effect of the incubation is reduced more and more.

A more comprehensive model could be developed, furthermore, from this bulk model, to take into account also other channels of electron loss, for instance the electron emission out of the target and transient (fast decaying) defect states.

Acknowledgements We would like to thank A. Semerok, O. Gobert and P. Martin from CÉA Saclay, France for the opportunity to use their equipment in the frame of a SLIC project and for their assistance with the LIF experiments.

References

1. M. Henyk, D. Wolfframm, J. Reif, Nucl. Instrum. Methods. Phys. Res. B **166–167**, 716 (2000)
2. F. Costache, J. Reif, Thin Solid Films **453–454**, 334 (2004)
3. S.S. Mao, F. Quéré, S. Guizard, X. Mao, R.E. Russo, G. Petite, P. Martin, Appl. Phys. A **79**, 1695 (2004)
4. J.T. Dickinson, S.C. Langford, J.J. Shin, Phys. Rev. Lett. **73**, 2630 (1994)
5. R. Stoian, D. Ashkenasi, A. Rosenfeld, E.E.B. Campbell, Phys. Rev. B **62**, 13167 (2000)
6. N.M. Bulgakova, R. Stoian, A. Rosenfeld, I.V. Hertel, E.E.B. Campbell, Phys. Rev. B **69**, 054102 (2004)
7. A. Rosen, E. Westin, E. Matthias, H.B. Nielsen, J. Reif, Phys. Scr. T **23**, 184 (1988)
8. J. Reif, Opt. Eng. **28**, 1122 (1989)
9. K. Tanimura, Phys. Rev. B **63**, 184303 (2001)
10. M. Reichling, M. Huisinga, D. Ochs, V. Kempter, Surf. Sci. **402–404**, 145 (1998)

11. L.P. Cramer, T.D. Cumby, J.A. Leraas, S.C. Langford, J.T. Dickinson, J. Appl. Phys. **97**, 103533 (2005)
12. F. Costache, *Dynamics of ultra-short laser pulse interaction with solids at the origin of nanoscale surface modification*. PhD Thesis, ISBN 978-3-8322-6465-9, Shaker Verlag Aachen (2007)
13. R. Lindner, R.T. Williams, M. Reichling, Phys. Rev. B **63**, 075110 (2001)
14. L. Sudrie, A. Couairon, M. Franco, B. Lamouroux, B. Prade, A. Mysyrowicz, Phys. Rev. Lett. **89**, 186601 (2002)
15. B.C. Stuart, M.D. Feit, S. Herman, A.M. Rubenchik, B.W. Shore, M.D. Perry, Phys. Rev. B **53**, 1749 (1996)
16. U.O. Karlsson, F.J. Himpsel, J.F. Mora, F.R. McFeely, D. Rieger, J.A. Yarmoff, Phys. Rev. Lett. **57**, 1247 (1986)
17. P. Agostini, G. Petite, Contemp. Phys. **29**, 57 (1988)
18. C.B. Schaffer, A. Brodeur, E. Mazur, Meas. Sci. Technol. **12**, 1784 (2001)